The Astrophysical Journal, 588:557–565, 2003 May 1

OBSERVATION OF GeV SOLAR ENERGETIC PARTICLES FROM THE 1997 NOVEMBER 6 EVENT USING MILAGRITO

A. Falcone,[1,2] R. Atkins,[3] W. Benbow,[4] D. Berley,[5] M. L. Chen,[5,6] D.G. Coyne,[4] B. L. Dingus,[3] D. E. Dorfan,[4] R. W. Ellsworth,[7] L. Fleysher,[8] R. Fleysher,[8] G. Gisler,[9] J. A. Goodman,[5] T. J. Haines,[9] C. M. Hoffman,[9] S. Hugenberger,[10] L. A. Kelley,[4] I. Leonor,[10] J. F. McCullough,[9] J. E. McEnery,[3] R. S. Miller,[1] A. I. Mincer,[8] M. F. Morales,[4] P. Nemethy,[8] J. M. Ryan,[1] B. Shen,[11] A. Shoup,[10] G. Sinnis,[9] A. J. Smith,[5] G. W. Sullivan,[5] T. Tumer,[11] K. Wang,[11] M. O. Wascko,[9,12] S. Westerhoff,[9,13] D. A. Williams,[4] T. Yang,[4] and G. B. Yodh[10]

ABSTRACT

Milagrito was an extensive air-shower observatory that served as a prototype for the larger Milagro instrument. Milagrito operated from 1997 February to 1998 May. Although it was designed as a very high energy (few hundred GeV threshold) water-Cerenkov gamma-ray observatory, it could also be used to study solar energetic particles (SEPs). By recording scaler data, which correspond to photomultiplier tube singles rates, it was sensitive to muons and small showers from hadronic primary particles with rigidities above ~4 GV. Milagrito simultaneously recorded air-shower trigger data of primary particles with energies greater than ~100 GeV that provide the data to help reconstruct event directions. The Milagrito scalers registered a ground-level enhancement associated with the 1997 November 6 SEP event and X9 solar flare. At its peak, the enhancement was 22 times the background rms fluctuations. Based on comparisons to neutron monitor and satellite data, we find evidence that the rigidity power-law spectrum for the differential flux of energetic protons steepened above ~4 GV and that the acceleration site was high in the corona (at ~3 $R_\odot$ above the photosphere), assuming that a CME-driven shock was responsible for the ground-level enhancement.

Subject headings: acceleration of particles — interplanetary medium — Sun: flares — Sun: particle emission

1. INTRODUCTION

Particle acceleration to energies greater than 1 GeV due to solar processes is well established (e.g., Meyer, Parker, & Simpson 1956; Parker 1957). However, few data exist demonstrating acceleration of particles above 5 GeV (Chiba et al. 1992; Lovell, Duldig, & Humble 1998). The energy upper limit of solar particle acceleration is unknown, but it is important because it relates not only to the nature of the acceleration process, itself not ascertained, but also to the environment at or near the Sun where the acceleration takes place. Because of their small size and the low flux of protons at these energies, space-based instruments are relatively ineffective above ~1 GeV. However, neutron monitors become efficient at these energies. Neutron monitors provide an integral measurement of the particle intensity above a threshold determined by the altitude and geomagnetic location of the monitor (Debrunner 1994; Simpson 1957). As energy increases, the solar energetic particle (SEP) spectra typically fall faster than the effective areas rise for neutron monitors. This limits their application above several GV. Using the global network of neutron monitors, one can often extract proton spectrum information from the different count rates at neutron monitor stations at different geomagnetic cutoffs. This implies that little energy information exists in the neutron monitor data above ~14 GV, which corresponds to the cutoff of a sea-level equatorial station. In the past, underground muon telescopes have been used to study the higher energy SEPs, but their energy thresholds are far above that of neutron monitors, so they rarely register an event.

Milagro, as was its prototype, Milagrito, is capable of studying high-energy SEP events by operating at high energies with large areas. Milagro, as described below, is a ground-level water Cerenkov gamma-ray detector that is also sensitive to solar energetic protons at the top of the atmosphere. The energy threshold of Milagrito was lower than the thresholds of underground muon telescopes and traditional extensive air shower arrays, while its effective area was much larger than that of neutron monitors. Milagrito could detect a relatively large fraction of the secondary particles from air showers by utilizing the water-Cerenkov technique in a large, water-filled pond. This increased sampling of shower particles relative to that of traditional extensive air shower arrays, which are insensitive below the TeV regime, contributes to the lower energy threshold of Milagro and Milagrito for detecting SEPs. This technique also leads to an effective area that is more than 3 orders of magnitude greater than that of neutron monitors above ~4 GV. With an intrinsic rigidity threshold for vertical protons of

[1] Space Science Center, University of New Hampshire, Durham, NH 03824.
[2] Current address: Purdue University, West Lafayette, IN 47907; afalcone@physics.purdue.edu.
[3] Physics Department, University of Wisconsin, Madison, WI 53706.
[4] Physics Department, University of California, Santa Cruz, CA 95064.
[5] Physics Department, University of Maryland, College Park, MD 20742.
[6] Current address: Brookhaven National Laboratory, Upton, NY 11973.
[7] George Mason University, Fairfax, VA 22030.
[8] Physics Department, New York University, New York, NY 10003.
[9] Los Alamos National Laboratory, Los Alamos, NM 87545.
[10] Physics Department, University of California, Irvine, CA 92717.
[11] Physics Department, University of California, Riverside, CA 92521.
[12] Current address: Louisiana State University, Baton Rouge, LA 70803.
[13] Current address: Columbia University, New York, NY 10027.

~3.9 GV, due to the location of the detector within the Earth's geomagnetic field, Milagro/Milagrito measurements complement those of the neutron monitor network. An increased sensitivity to high-energy, anisotropic events can also be achieved when Milagro/Milagrito is able to reconstruct incident directions of the primary particles.

Coronal mass ejections (CMEs) and solar flares are frequently accompanied by SEPs, but the details of the acceleration process(es) continue to elude researchers. Although SEP events are frequently categorized as either gradual or impulsive (Lee 1991; Reames 1999; Gosling 1993), some events do not seem to fit neatly into either category (Möbius et al. 1999). Gradual events generally exhibit greater fluxes of SEPs over long timescales and tend to be associated with long-duration type II/IV radio emission, corona-like ion abundances, and low electron-to-proton ratios. On the other hand, impulsive events typically exhibit smaller fluxes of SEPs over shorter timescales. They also tend to be associated with large electron-to-proton ratios and enhancements in heavy ions and ^{3}He. Fast (>400 km s^{-1}) CME-driven coronal and interplanetary shocks are generally thought to be the accelerating agent for the gradual events (Lee 1997; Kahler 1992), while the impulsive events are generally thought to originate at the flare sites (Reames 1999).

On 1997 November 6 at 11:49 UT, an X9 flare with an associated CME occurred on the western hemisphere (63W) of the Sun. The flare and the CME were well observed by many instruments, and the interplanetary particles exhibited both gradual and impulsive characteristics. The *GOES-9* satellite detected energetic protons in excess of 100 MeV, and hard X-rays were detected by *GOES-9*[14] and the *Yohkoh* HXT (see Sato et al. 2000). *Yohkoh* also recorded impulsive gamma-ray emission up to 100 MeV for approximately 5 minutes, along with the presence of gamma-ray lines (Yoshimori et al. 2000a). LASCO detected the launch of the CME from the Sun, and the speed of the leading edge was estimated to be between 600 and 2200 km s^{-1} (Leblanc et al. 2001; C. St. Cyr 2001, private communication; Zhang et al. 2001). Metric radio emission was also observed during this event (Maia et al. 1999). Using *Advanced Composition Explorer* (*ACE*) measurements, Cohen et al. (1999) and Mason et al. (1999) reported hard ion spectra above 10 MeV nucleon^{-1}. Furthermore, Fe and ^{3}He enhancements (^{3}He/^{4}He ~4 × coronal and Fe/O ~ 1) were evident in the interplanetary particle populations at these energies. These values are greater than those expected for a gradual event, but the enhancements are not as great as those found in many impulsive events.

Many instruments in the worldwide network of neutron monitors registered a ground-level enhancement (GLE) in response to protons with energies in excess of ~1 GeV (Duldig et al. 1999). The rate increase began shortly after 12:00 UT with an anisotropic component, but the distribution approached isotropy by the time of maximum, approximately 45 minutes after the onset (Lovell et al. 2002). Low-latitude monitors, such as Mexico City (cutoff rigidity 8.6 GV), did not record an increase. The Climax neutron monitor, located less than 400 km north of the Milagrito site with a vertical cutoff rigidity of 3 GV, was among those to record an increase.

[14] *GOES* data are available at: http://www.sec.noaa.gov/ftpdir/plots/1997_plots/proton/971106.gif.

2. MILAGRITO INSTRUMENT DESCRIPTION

Milagrito was located near Los Alamos, New Mexico, at an elevation of 2650 m (750 g cm^{-2} atmospheric overburden). It operated as a prototype for the Milagro instrument from 1997 February to 1998 May (Atkins et al. 2000; McCullough et al. 1999). The detector was composed of 228 upward-facing photomultiplier tubes (PMTs) submersed in 1–2 m of clean water (attenuation length of about 5 m for 350 nm light). These tubes were placed within an 80 × 60 × 8 m pond, under a light-tight cover, in a square grid pattern with 2.8 m spacing between adjacent PMTs. When an energetic hadronic particle or gamma ray is incident on the Earth's atmosphere, it can induce an extensive air shower (EAS) that propagates downward in the form of a thin (~1–3 m) "pancake-like" plane of relativistic secondary particles. Upon entering water, the charged particles from the EAS emit Cerenkov light in 42° cones. These Cerenkov photons were then detected in Milagrito by the PMT array. The gamma rays in the EAS undergo Compton scattering and pair production when they enter the water, producing additional Cerenkov radiation. With this technique, a large fraction of the shower particles striking the pond are detected, resulting in a large effective area.

Designed as a very high energy (VHE) gamma-ray observatory, the Milagrito air-shower trigger was sensitive to extensive air showers from primary hadrons and gamma rays above ~100 GeV. Milagrito required at least 100 PMTs to register signals in coincidence in order for the data-acquisition hardware to record an air-shower trigger event. For a PMT to contribute to this trigger, its pulse height had to exceed a threshold corresponding to ~0.25 photoelectrons, referred to as the low threshold. For each event, the time and pulse height in each PMT were recorded. The time-over-threshold technique was used to measure pulse height. Once these data were recorded, they could be used to reconstruct the incident direction of the primary particle with a resolution less than 1°. The hadron-induced showers were treated as background for the studies of gamma-ray sources using the air-shower trigger data, but hadron-induced events were treated as a signal for the purposes of solar and cosmic-ray physics.

In addition to recording these air-shower trigger events (telescope mode), Milagrito also recorded scaler data that correspond to PMT singles rates. These data are similar to those of a neutron monitor. The value that is recorded is a time-integrated measurement of the rate of single-PMT hits in the pond. For the purposes of this scaler counting, a PMT was considered to be hit when its pulse height exceeded a threshold corresponding to ~7.6 photoelectrons, referred to as the high threshold. These high-threshold data have smaller background fluctuations than the low-threshold data used for the air-shower trigger. This is important when considering the large number of smaller and unreconstructable events registered by the scalers. The PMTs were separated into 15 4 × 4 patches. Each of these patches contained 16 PMTs. The high-threshold output from each of the 16 PMTs went through a logical "OR"; thus, the high-threshold scalers counted the number of patches that registered at least one hit. Since the PMT signals went through a logical OR, a patch with multiple PMT hits within ~45 ns of each other would register only one count. The number of scaler counts was recorded with a frequency of 1 Hz.

Since the energy range most likely to be of primary interest to solar physics is below 100 GeV, the scaler counting ability of Milagrito is useful, despite the fact that reconstruction of event directions is not possible with these data. By recording these scaler data, an integral measurement above a hardware-defined threshold was performed. These data provide a high-energy complement to the network of neutron monitors.

Using Monte Carlo calculations, the effective area of the Milagrito instrument was computed. For the purpose of simulating the Milagrito response, the effective area is defined as $(N_{\rm trigger}/N_{\rm throw})A_{\rm throw}$, where $A_{\rm throw}$ is the area over which the shower core is thrown and $N_{\rm trigger}$ and $N_{\rm throw}$ are the number of triggers and the number of primary particles thrown, respectively. Of particular interest for solar ground-level events is the effective area of Milagrito for protons incident isotropically on the atmosphere, at zenith angles ranging from 0° to 90° (Fig. 1). The curves shown in the figure correspond to the effective areas of the high-threshold scalers and the air-shower trigger. The effective area from 60° to 90° was estimated by extrapolating the area curve from the 0°–60° range as computed with the Monte Carlo code (see below). In the absence of effects specific to large zenith angles, the overwhelming majority of the contribution to the scaler efficiency comes from zenith angles below 60°. An example of the relative contribution at angles within 60° of the zenith for protons at 50 GeV can be seen in Figure 2. Since cosmic-ray showers were not simulated between 60° and 90° because of limitations of the software and time, effects that are present only at large zenith angles are not reflected in these effective area curves (see § 3.2). While this could have a significant impact on the analysis of the air-shower data, which may be more prone to unsimulated effects specific to high zenith angles, we do not expect it to significantly affect the scaler data.

The complete simulation of the detector response was performed in two steps (Atkins et al. 2000). The initial interaction of the primary particle with the atmosphere and the generation of secondary particles was simulated with the CORSIKA air-shower simulation code (Heck et al. 1998). The primary particles and shower particles are tracked through the atmosphere, which is stratified into five horizontal layers. When the particles initiate a reaction or decay, the secondary particles are also tracked through the atmosphere. Electromagnetic interactions are simulated using EGS4 code. For the hadronic interactions, the VENUS code is used at high energies, and GHEISHA is used at low energies (<80 GeV). The second step was to simulate the response of the detector itself using GEANT (CERN 1994).

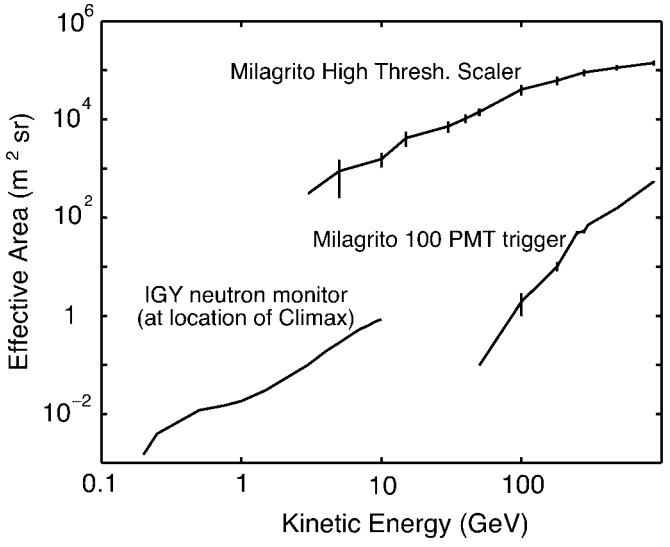

FIG. 1.—Effective area of Milagrito to isotropic protons incident at the top of the Earth's atmosphere compared to that of an international geophysical year (IGY) neutron monitor. The vertical error bars are statistical. The error is largest at low energies because of the low efficiency of the detector.

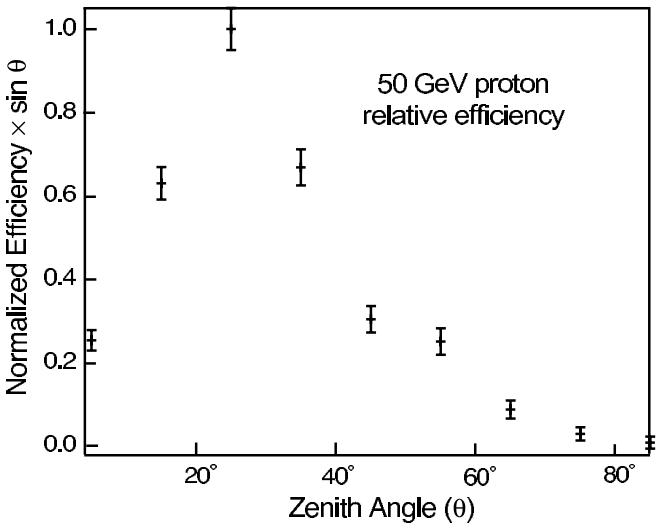

FIG. 2.—Relative contribution of 50 GeV protons to Milagrito scalers normalized to 25° and plotted vs. zenith angle. The sin Θ factor represents the larger solid angle at large zenith angles. Points beyond 60° are a polynomial (× sin Θ) extrapolation from smaller Θ. The expected contribution from Θ > 60° is seen to be small.

The areas in Figure 1 were calculated using Monte Carlo events whose shower cores were thrown randomly over a large area surrounding the Milagrito pond. To ensure that the Monte Carlo showers were thrown over a large enough area, we progressively increased the throw area until the effective area reached an asymptotic value. This occurred at approximately 7000 × 7000 m^2. Figure 3 illustrates the relationship between the calculated Milagrito effective area and the shower-core throw area for 50 GeV protons. We note that the effective area of the Milagrito scalers has a significant contribution from hadronic showers with cores far (>3 km) from the detector. This effect increased the estimated effective area at ~5–100 GeV by ~3 orders of magnitude relative to earlier estimates, which used a throw dimension of 100 m (Falcone et al. 1999; Ryan et al. 1999).

To estimate the systematic errors in the instrument response, we folded the cosmic-ray spectrum at the top of the atmosphere through the calculated response. This results in a theoretical value for the instrumental scaler rate due to Galactic cosmic rays, which comprise most of the Milagrito background rate. The measured background scaler rate in Milagrito is ~30% of this predicted value. While this provides us with a level of confidence in the calculated effective area curves, there are still some concerns. When GHEISHA is used to simulate showers initiated by particles with energies below ~20 GeV, it is possible that the sum of the secondary shower particle energies can be as

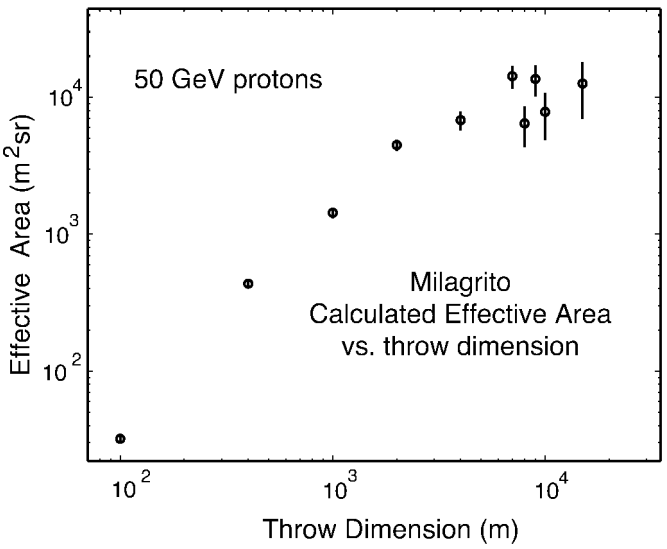

FIG. 3.—Relationship between the calculated effective area of the Milagrito scalers and the spatial dimension over which the simulation is computed. The calculated area increases with the square of the throw dimension near the instrument. The size of the error bars increases at large throw dimensions because of poor statistics. The y-axis has arbitrary scaling.

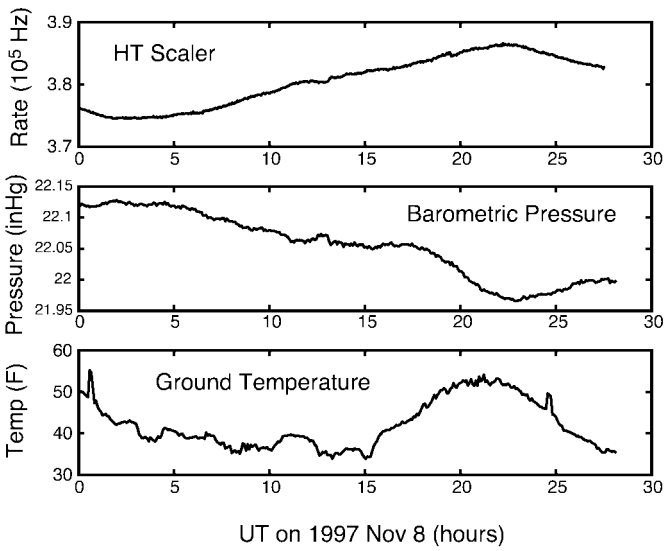

FIG. 4.—Typical diurnal fluctuations in Milagrito scaler rate during a period (1997 November 8) relatively free of instrumental effects.

much as 20%–30% greater than the energy of the primary hadron (D. Heck 1999, private communication). This may be the source of the systematic error that results in the factor of 3 difference between the measured cosmic-ray rate and the predicted rate. However, as we show in § 4, this systematic error has only a small effect on the deduced solar proton power-law spectrum.

At 10 GeV, the high-threshold scaler effective area of Milagrito was ~3 orders of magnitude greater than that of a sea-level neutron monitor, with the Milagrito effective area rising rapidly with energy. The threshold of Milagrito is determined by the combined effects of the geomagnetic field and atmospheric attenuation. The effects of the atmosphere are included in the effective area curves for zenith angles between 0° and 60°, while larger angles are assumed to be a simple extrapolation of the curve, as depicted in Figure 2. The geomagnetic effect is incorporated by assuming a hard cutoff at the calculated vertical cutoff rigidity, i.e., ~3.9 GV. The true cutoff is actually a function of azimuth, zenith angle, and magnetic field fluctuations, but these effects are not included.

To interpret the scaler data of Milagrito properly, one must first correct the ground-level scaler rates for atmospheric pressure, temperature, and other diurnal effects (Hayakawa 1969). Typical background cosmic-ray rate fluctuations on a timescale of ~1 day are shown in Figure 4. This figure also shows the barometric pressure at ground level. One can clearly see the increase in background rate as the pressure, and consequently the atmospheric overburden, decreases on the order of 10%–20% per kPa. Ground-level atmospheric temperature also affects the background rate by varying the muon lifetime. Although this effect cannot be seen in the figure because of the large pressure variation, the overall temperature effect can cause variations on the order of 9×10^{-2} percent per °C. Preliminary and incomplete estimates of these correction factors for Milagro/Milagrito were computed based on observations. They are reasonably consistent with earlier work (Fowler & Wolfendale 1961). (Fortunately, these atmospheric effects have only a small effect on fast transient events.) Accurate estimates of the pressure and temperature correction factors for Milagrito were not calculated because there was no sufficiently long period with a uniform operating mode near the time of the GLE. Milagrito was an engineering prototype that had significant changes in detector parameters such as water level, electronic thresholds, and light-leak integrity of the cover.

3. OBSERVATIONS OF 1997 NOVEMBER 6 EVENT USING MILAGRITO

Since their sensitivities are different, the scalers and the air-shower triggers are analyzed separately.

3.1. *Scaler Observations*

Milagrito measured a scaler rate increase coincident, within error, with the increase observed by the Climax neutron monitor (see Fig. 5). If one accounts for the background meteorological fluctuations, the event duration and time of maximum intensity as seen with Milagrito are also consistent with those of Climax. The magnitude of the scaler rate increase is ~22 times the rms fluctuations of the instrument background using 160 s time bins (this binning was chosen because the data stream used for this analysis is binned similarly). The background scaler rate prior to the event was ~375 kHz, and the event produced a rate increase of ~0.5%. The rms of observed background fluctuations during a 2 hr period prior to the event onset was 84 Hz. This is nearly twice that expected from Poisson statistics. These larger fluctuations may be a result of effects such as meteorological fluctuations in the upper atmosphere and at the Milagro site. Regardless of the source, or sources, of these fluctuations, we estimated the chance probability of an increase of this magnitude, over this time frame, by examining the data over the lifetime of Milagrito, by binning all of the Milagrito high-threshold scaler data into 10 minute intervals. We then calculated the difference between the average rate in any two time bins separated by 1 hr from the

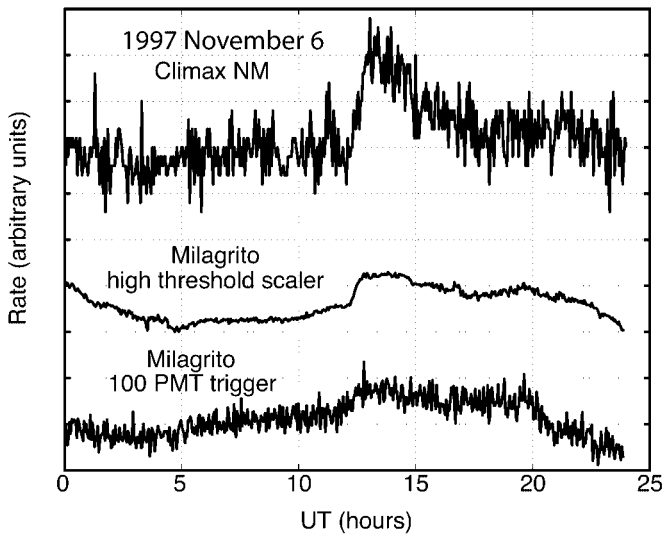

FIG. 5.—Milagrito high-threshold scaler rate and air-shower trigger rate plotted with those of the Climax neutron monitor. Within uncertainties, the high-threshold scaler rate increase of Milagrito coincides with that of Climax. Diurnal background variations are also apparent in the Milagrito data. (Climax data courtesy of C. Lopate, University of Chicago).

start of one bin to the start of the next. There were only two other rate increases of at least this magnitude during the 15 month (no data recorded for ~20% of this time due to maintenance, hardware reconfigurations, etc.) lifetime of the instrument. One of these is a possible light leak, and the other was a power-up transient effect. We thus estimate that the probability upper limit for rate increases, for any reason, with a magnitude and timescale similar to that of the 1997 November 6 event is $\sim 2 \times 10^{-4}$. This number represents the upper limit of the probability of registering a random rate fluctuation of this magnitude over the entire lifetime of Milagrito (including all of its systematics), whereas the $22 \times$ rms rate increase was well correlated in time with other GLE detections.

The scaler rate plotted in Figure 5 does not include one of the 15 patches of the detector. This historically noisy group of PMTs, located within patch 7, exhibited an unrelated instrumental rate increase a few hours after the onset of the CME related rate increase. This type of instrumental rate increase (commonly referred to as "flashing" and thought to be caused by arcing in the base or light emission in the tube) was common in some clusters of PMTs, but these effects are easily identified. A "flasher" will cause a disproportionate rate increase in a local cluster of PMTs, but an air shower signal will produce a more uniform increase over the entire pond. During the rate increase on 1997 November 6, all of the patches except for patch 7 experienced a uniform rate increase with an average increase of 0.48% and a standard deviation of 0.08%. However, patch 7 experienced a rate increase of (1.10 ± 0.03)%. We therefore removed the contribution from patch 7 from the analysis and from the data plotted in Figure 5.

3.2. *Air-Shower Trigger Observations*

The air-shower trigger rate at the time of this event is also shown in Figure 5. It is designated as the 100 PMT trigger rate, since an air-shower trigger requires that 100 PMTs register a signal for a single event. Once this threshold has been exceeded the data are individually recorded. The recorded data includes the identifications of the PMTs that triggered and their relative signal times. This mode is the main mode for TeV gamma-ray astronomy. In order for a gamma ray or a vertically incident proton to surpass this threshold, its energy must be greater than ~100 GeV.

An air-shower trigger rate increase coinciding with the onset of the Climax GLE is apparent. If real, it potentially represents the detection of very high energy solar energetic protons. The magnitude of the air-shower trigger rate increase is approximately twice the rms fluctuations of the background using 160 s time bins, the same timescale used for the scalers (rms is calculated using several hours of data immediately prior to the event onset). Another estimate of the significance that considers longer timescales was obtained by finding the rms fluctuations on larger timescales and on several days in November. By examining the rms fluctuations in 1 hr time bins between 10:00 and 17:00 UT for six days in November, we found that the air-shower trigger event rate excess was ~1.3 times the fluctuations. Although it seems coincidental that such a fluctuation, being either instrumental or statistical, occurred at the time of the Climax increase and the Milagrito scaler increase, we considered this possibility and also the possibility that the increase in the air-shower trigger rate is due to the solar particle event. If the increase is due to the same solar particles that caused the scaler rate increase, then it requires a much harder spectrum than that derived from neutron monitor data and the scaler rate increase of Milagrito, with large particle fluxes above ~100 GeV. However, the simulations used to calculate the effective areas in Figure 1 did not directly compute the physics of particle transport near horizontal viewing angles, but rather extrapolated from higher zenith angle calculations. Conceivably, a reaction channel exists for producing detectable muons near the horizon from lower energy protons incident at the top of the atmosphere. If these high zenith angle muons contributed to the air-shower trigger apparent rate increase, they would have been the result of high-energy proton primaries (>30 GeV), based on estimates of muon losses in the atmosphere. The effective area curve in Figure 1 would not apply to this triggering mechanism. In order to determine the spectrum of the primary protons associated with this mechanism, extensive simulations must be performed to investigate the instrument air-shower trigger response to primary particles beyond 60°.

Instrumental effects were also investigated. This apparent shower trigger rate increase does not appear to conform to known instrumental effects. One potential source for an instrumental rate increase is a temperature variation in the electronics boards. However, the temperature of the electronics in Milagrito was monitored, and no correlation between variations of board temperature and trigger rate was evident during this event. Another potential source for an instrumental rate increase is "flashing" PMTs. Flashers, which are caused by light emission at the base and/or in the tube of the PMT, are a common problem with water Cerenkov detectors. Based on an analysis of the signatures of flashers in the Milagrito data, we conclude that they are not responsible for the apparent air-shower trigger rate increase.

We are therefore left with three possibilities: (1) the air shower trigger "signal" is due to the solar particles that caused the scaler rate increase and the neutron monitor

increase, representing a radically hard solar proton spectrum; (2) the air shower trigger "signal" is a random occurrence of an unusual, but not impossible, fluctuation; or (3) the air shower trigger "signal" comes from a detection mode of the instrument for which the response of the instrument is not fully understood. For the air-shower trigger data to be consistent with data from the scaler mode and from other instruments, we must conclude that the increase is either random or a not understood response of the instrument to low-energy solar protons. Therefore, for the remainder of the discussion, we do not consider the apparent increase in the air-shower trigger rate to be due to the same solar protons that can be analyzed using the effective area curves in Figure 1. Future work may investigate the response of the air-shower trigger mode to alternative mechanisms, such as high zenith angle muons, but these studies are beyond the scope of this paper. The spectrum that we derived and discuss below is based solely on the high-threshold scaler data and data from neutron monitors.

4. PROTON SPECTRUM BASED ON MILAGRITO AND NEUTRON MONITOR DATA

Using only the high-threshold scaler rate increase of Milagrito, we can derive characteristics of the primary proton spectrum. We did this by folding a trial power-law spectrum of protons through the response (including the Earth's atmosphere) of the instrument. The trial power-law spectrum is of the form

$$f = C\left(\frac{P}{P_0}\right)^{-\alpha}, \quad (1)$$

where P is rigidity (GV), f is the differential proton flux (m^{-2} s^{-1} sr^{-1} GV^{-1}), and $P_0 = 1$ GV. The expected rate increase in the detector, for a given C and α, is then found by integrating

$$R = \int_{P_{\rm cutoff}}^{\infty} f(P) A_{\rm eff}(P)\, dP\ , \quad (2)$$

where $A_{\rm eff}$ is the proton effective area of Milagrito as described in § 2. The parameters of the trial spectra, C and α, are then varied until a good fit to the measured rate increase is achieved. By only using the high-threshold scaler rate in this analysis, a range of acceptable pairs of C and α was determined. To uniquely determine the parameters, another detector with a different response is necessary.

We made the assumption that the geomagnetic rigidity cutoff can be accurately represented by a single value, namely, the vertical cutoff rigidity of 3.9 GV. This ignores any fluctuations in the interplanetary magnetic field, as well as the variation in the cutoff with zenith angle and azimuth. In addition, although not the case early in the event, we take the pitch angle distribution of protons from the event to be isotropic for purposes of modeling the proton flux. Within ~15 minutes of the onset of the event, at 12:30 UT, the FWHM of the pitch angle distribution was measured by Lovell et al. (2002) to be ~60°, and by ~13:30, at which time the rate increase was at a maximum, the pitch angle distribution FWHM was ~210°.

After obtaining the range of spectral parameters from the Milagrito data, we compared this to the spectrum obtained with the worldwide network of neutron monitors. Neutron monitor data for this proton event, near the time of maximum intensity (starting at ~12:45–13:00 UT), indicate a rigidity power-law spectral index between approximately 5.2 and 6 in the 1–4 GV rigidity range (Duldig & Humble 1999; Lovell et al. 2002). If the Milagrito-derived range of spectral parameters for protons above 4 GV is required to match the neutron monitor flux at 4 GV and if we assume an unbounded power law above 4 GV, then a unique solution for the spectrum above 4 GV exists. Doing this, we found that the spectral index, α, that best fits the data is 9.0 ± 2.3. The statistical error bars for the spectral parameters are obtained by varying the input parameters by their $1\,\sigma$ error bars. The error is dominated by the error in the calculated effective area. Statistical errors from background fluctuations and errors arising from the fitting technique are also included, but they are small compared to the effective area error. Based on the comparison of the measured cosmic-ray rate to that predicted by the calculated effective area, the known systematic error for such a power-law index is 0.6. In this analysis, we assumed that the spectrum is a simple power law above 4 GV. We also repeated the analysis with a sharp upper rigidity cutoff in the neutron monitor proton spectrum, rather than joining different power-law spectra as described above. We considered this spectral cutoff to be a free parameter while extending the spectrum derived from the neutron monitors up into the energy range of Milagrito. Our analysis shows that in order for the Milagrito scaler data and the neutron monitor data to be consistent, the sharp cutoff must occur at 4.7 ± 0.5 GV (effective area error as described above), if we assume that the $P^{-5.2}$ spectrum of Lovell et al. (2002) extends into the energy range of Milagrito.

Both of the cases described above are illustrated in Figure 6, along with the proton spectral data from neutron monitors just below 4 GV. These results constitute evidence for a cutoff above the Milagrito threshold or a rollover in the spectrum. This is most likely of the form of a progressive spectral softening throughout the rigidity range above ~1 GV.

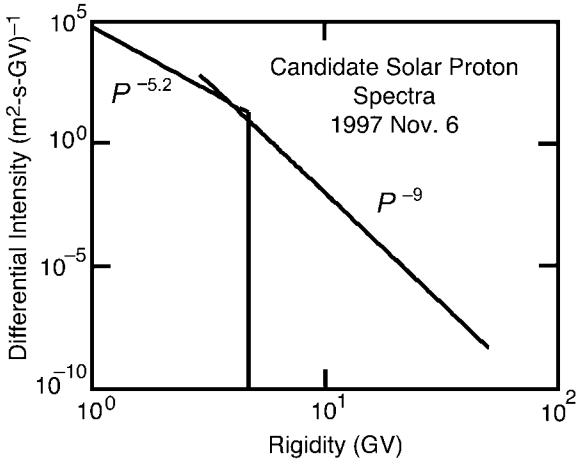

FIG. 6.—Calculated differential flux of isotropic protons from the 1997 November 6 SEP event. The spectrum below 4 GV comes from the worldwide neutron monitor network. Above 4 GV, two possible spectra that are consistent with the Milagrito high-threshold scaler rate increase are shown and described in the text. The circle denotes the energy where the neutron monitor and the Milagrito spectra must overlap.

5. EVENT TIMING

Prior to the detection of energetic particles at Earth, X-rays and gamma rays were detected by space-based instruments. The CME-associated solar flare was categorized as X9. Yoshimori et al. (2000b) reported the detection of gamma rays up to 70 MeV, with an onset time of 11:52 UT for the 10–20 MeV emission (see Fig. 7). Several lines were present in the spectrum derived from *Yohkoh* data, including the 2.223 MeV neutron-capture line and 4.4 MeV C and 6.1 MeV O deexcitation lines. By virtue of the line detection, we know that proton acceleration was present at the flare site between 11:52 and 11:57 UT. The gamma-ray event, as measured with *Yohkoh*, was finished within 5 minutes of onset.

The time profile measured by Milagrito is consistent with that of Climax, with allowances made for the long-term meteorological fluctuations (Figs. 4 and 5). The onset of the Milagrito scaler rate enhancement was at 12:12 UT $\pm$ 6 minutes. While the uncertainty in the Climax onset time is certainly larger than that for Milagrito, it can be seen from Figure 7 that the two onset times are simultaneous within the error. The times of maximum intensity and the duration are also similar, although we cannot precisely locate the end of the event in the Milagrito data because the rising background rate meets the falling solar signal. The rate in the Milagrito scalers, during the increase, reached its maximum value between 12:44 and 13:00 UT (The value reported here is actually the time that the rate reached the maximum value after which the rate plateaued. So, the time of maximum could actually be as much as an hour beyond this value.) The *GOES* satellite also observed an enhanced rate of protons from this event with the >100 MeV proton event lasting for more than two days. *GOES* also detected protons from an event that occurred on November 4. While the flux of >100 MeV protons had returned to the predisturbance level by the time of the November 6 event, the flux of >10 MeV protons was still elevated by a factor of ~10 over its intensity prior to the November 4 event.

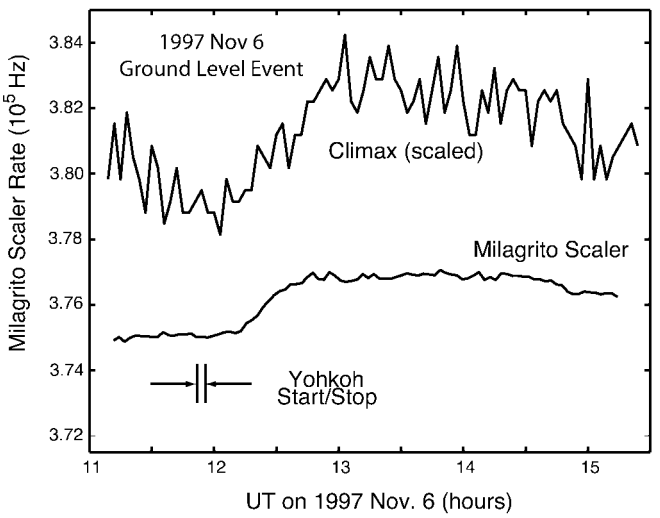

FIG. 7.—Onset of the Milagrito high-threshold scaler increase and the Climax increase. The beginning and end of the *Yohkoh* γ-ray line observations are indicated.

6. DISCUSSION AND CONCLUSIONS

When the short duration (~5 minute) of the gamma-ray line emission and the long duration (several hours) of the high-energy GLE proton acceleration are considered, it becomes difficult to attribute the GLE proton acceleration to the flare. Although this analysis, by itself, does not rule out acceleration at the flare site with subsequent interplanetary diffusion, this scenario is not likely. The very different rise time and duration of the Milagrito signal are not consistent with a single diffusion time in the corona or interplanetary space if we take the gamma-ray time profile to be indicative of the proton acceleration interval. One needs rapid diffusion and an anomalously long path length early to achieve the delay and the abrupt onset with slow diffusion thereafter to prolong the event.

It is also not possible that the solar flare particles as manifested in the gamma-ray flare are responsible for the ground-level event. The approximate expression for the expected velocity dispersion of anisotropic flare particles reaching the Earth is $\Delta t = 1.3\ \mathrm{AU}/v - 8.3$ minutes (Kahler 1994), where v is the particle velocity and the distance of 1.3 AU includes the extra path length due to the proton pitch angle. This path length is shown to be realistic in the following discussion. Using the velocity of 5 GV protons, one would expect a time difference of ~167 s, whereas we measure ~1200 s between 11:52 and 12:12 UT. A simple and likely explanation is that of an extended CME shock front being responsible for the acceleration and transport of the protons in interplanetary space. In this scenario protons are accelerated at the flare site during the impulsive phase, but the GLE protons, which come later, are probably accelerated higher in the corona many minutes after the end of the impulsive phase, as seen in the 70 MeV gamma-ray data.

If a CME-driven shock was responsible for the GLE protons, then the height of the CME at the time at which protons reached these high energies and escaped can be estimated by looking at the time difference between the launching of the CME (often taken to be the impulsive phase of the flare) and the GLE onset, while accounting for the proton path length along the nominal Parker spiral of the interplanetary magnetic field produced by a 350 km s^{-1} solar wind (F. M. Ipavich 2001, private communication). A path length of 1.17 $\pm$ 0.05 AU from the region around the flare site to Earth during the time of the 1997 November 6 event is expected from a 350 km s^{-1} solar wind if any interplanetary magnetic field (IMF) disturbances are neglected (the wind speed error dominates the error bars). The path length also depends on the pitch angle of the particles. The path length increases by sec Θ, where Θ is the pitch angle of the proton. Although the event was nearly isotropic by the time of maximum rate, the onset time of the event is determined by the earliest arriving particles, which were the ones with small pitch angles that were beamed along the IMF line. The FWHM of the pitch angle distribution was approximately 60° at 12:30 UT, but it is reasonable to assume that the event was more anisotropic at the time of onset (Lovell et al. 2002).

In computing the position of the GLE protons at the time of their release, we assumed that the CME was launched at the solar surface with an instantaneous velocity of 2100 $\pm$ 50 km s^{-1} (using the visual measurement of Zhang et al. 2001) at 11:52 UT (as observed from Earth, or 11:44

after correcting for light propagation). The launch time was estimated by linearly extrapolating the CME position curve (obtained from LASCO data) back to 1 solar radius. Typically, this places the launch time too late unless one accounts for acceleration, but Zhang et al. (2001) concluded that there was a very rapid acceleration for the 1997 November 6 CME, which we take to be infinite. We furthermore assumed that the Milagrito signal was produced by 5 ± 1 GV protons. Since we only know the pitch angle distribution at times later than 12:30, which is more than 15 minutes after the onset, we computed the proton release height for three values of average pitch angle: 0°, 20°, and 40°. Based on the pitch angle distribution observations of Lovell et al. (2002) and the fact that the onset time is determined by the particles with the smallest pitch angles, we consider 20° to be a reasonable value for the mean pitch angle. With the center of the Sun as the coordinate system origin, the proton release distance x_1 is

$$x_1 = (\Delta t + 8.3 \text{ minutes}) v_c - x_2 \left(\frac{v_{\rm CME}}{v_p} \right) + x_0 \ , \qquad (3)$$

where x_0 is the solar radius, x_2 is the total length of the proton path from time of release to Earth including the Parker spiral and the $\sec \Theta$ factor, Δt is the measured time difference between the observation of the CME launch and the GLE onset, v_p is the proton velocity, and $v_{\rm CME}$ is the CME speed (assumed to be constant). The greatest uncertainty in this calculation is in Δt, which we take to be ± 360 s, i.e., the 6 minute uncertainty in the onset time. However, including all the uncertainties listed above we obtain a proton release heliocentric radius of 4.3 ± 1.1, 4.2 ± 1.1, and 4.8 ± 1.1 $R_\odot$, using mean pitch angles of 0°, 20°, and 40°, respectively. This corresponds to 3.2 ± 1.1 $R_\odot$ above the photosphere, assuming a mean pitch angle of 20°.

This spatial scale is consistent with published results on GLE ion acceleration heights found for the 1990 May 24 CME event studied by Lockwood, Debrunner, & Ryan (1999) and the 1989 September 29 event studied by Kahler (1992). In these studies, which made use of similar timing arguments, particle injection heights were calculated to be ~ 2 $R_\odot$ and ~ 2.5–4 $R_\odot$, respectively.

The delay between the CME launch and the proton acceleration and release is also consistent with theory. An acceleration time of $\sim$10 minutes for $\sim$1–10 GeV protons is consistent with the collisionless shock model of Lee & Ryan (1986), assuming an injection energy of $\sim$10 MeV. In that model, the ratio of injection energy to accelerated particle energy as a function of time was calculated. While being a simple blast wave model, similar driven shock models could be applied (e.g., Lee 1997). Based on *GOES* data, there was an abundance of $>$10 MeV protons from the November 4 solar event that occupied interplanetary space. These ambient energetic protons could have provided the $>$10 MeV particle injection energies needed by the propagating CME-driven shock, although the seed particles could have come from other sources, such as the flare itself. This idea is consistent with the hypothesis that remnant solar particles from the earlier November 4 event were responsible for the unusual composition and charge states in this event (Mason et al. 1999). However, it is also consistent with the direct and prompt injection of several MeV protons and ions from impulsive, i.e., flare, particles within the 1997 November 6 event (Cliver et al. 2001).

Between 10 and 60 MeV, the instruments on board the *ACE* satellite observed a proton spectrum of the form $E^{-2.1}$ (Cohen et al. 1999), while at higher energies, ground-based instruments observed much softer spectra. The Milagrito data, combined with neutron monitor data, leads to a proton spectrum with a rigidity power law defined by $P^{-9.0 \pm 2.3}$, if a single power law is assumed above 3.86 GV (with an additional systematic error of 0.6 on the spectral index). A continuation of the $P^{-5.2}$ spectrum from Lovell et al. (2002) with a hard cutoff is also possible. These spectra are, by construction, continuous with the spectrum derived from the worldwide neutron monitor network at 4 GV. In any case, the spectra derived from Milagrito and neutron monitor data provide evidence for a gradual rollover or a cutoff somewhere in Milagrito's sensitivity range above 4 GV.

This steepened high-energy spectrum is also consistent with a low corona origin based on the implied shock strength. For a differential rigidity power-law spectral index of 9.0 ± 2.3 for relativistic protons to result from diffusive shock acceleration with planar geometry, one must have a shock compression ratio of $\sim$1.2 (M.A. Lee 2000, private communication). For a fast CME, such as this, to drive a shock with this low compression ratio, the Alfvén speed in the local medium must be high. This shock compression ratio implies an Alfvén speed higher than that expected in the solar corona. This implies that the acceleration occurred low in the corona, where the magnetic field and the Alfvén speed were large. This is consistent with the timing arguments presented above for a low coronal origin. Zank, Rice, & Wu (2000) and Lee (2000) predict shock-accelerated proton spectra that are steepened at high energies by the finite lifetime or three-dimensional geometry of the shock, in which case the compression ratio is probably much greater than what is suggested by the power-law index determined in this analysis.

The Milagro instrument, for which Milagrito was a prototype, is currently taking data (Sullivan et al. 2001). With its increased number of PMTs, multiple-layer design, increased effective area, and stable operation (relative to the engineering mode operation of Milagrito), Milagro may provide exciting results in the future. The number of PMTs in Milagro has increased to 723, compared to the 228 PMTs in Milagrito. These PMTs are arranged in two layers and they cover more physical area than was previously covered by Milagrito. Milagro's second layer of PMTs, submerged under 6.5 m of water, can provide the ability to reconstruct the directions of single muons and small showers in the pond. In the future, this second layer could also be used to incorporate advanced triggering mechanisms. Penetrating muons can be identified by using the pulse height information from this bottom layer of PMTs. Timing information can then be used to reconstruct the incident direction of these muons. This technique will lower the energy threshold for reconstructable events. Proposed enhancements to the data-acquisition system, which would allow Milagro to record this higher rate data and reconstruct hadronic events down to primary energies of $\sim$3 GeV, may further increase the Milagro capabilities, particularly its ability to study solar energetic particles (Ryan et al. 2000).

We acknowledge the contributions of many people who helped construct and operate Milagrito. In particular, we thank R. S. Delay, M. Schneider, and T. N. Thompson, who were indispensable during the construction, mainte-

nance, and operation of the detector. We also thank E. Cliver, J. Gosling, M. Lee, and J. Lockwood for their helpful comments and discussions. This work was supported in part by the National Science Foundation, the US Department of Energy Office of High Energy Physics, the US Department of Energy Office of Nuclear Physics, Los Alamos National Laboratory, the University of California, the Institute of Geophysics and Planetary Physics, the Research Corporation, the California Space Institute, and the University of New Hampshire Space Science Center.

REFERENCES

Atkins, R., et al. 2000, Nucl. Instrum. Methods Phys. Res., 449, 478
CERN Application Software Group. 1994, CERN Program Library Long Writeup W5013, Version 3.21
Chiba, N., et al. 1992, Astropart. Phys., 1, 27
Cliver, E. W., et al. 2001, in Proc. 27th Int. Cosmic-Ray Conf. (Hamburg), Vol. 8, ed. M. Simon, E. Lorenz, & M. Pohl (Katlenburg-Lindau: Copernicus Gesellschaft), 3277
Cohen, C. M. S., et al. 1999, Geophys. Res. Lett., 26, 149
Debrunner, H. 1994, in AIP Conf. Proc. 294, High Energy Solar Phenomena, ed. J. M. Ryan & T. W. Vestrand (New York: AIP), 207
Duldig, M. L., & Humble, J. E. 1999, in Proc. 26th Int. Cosmic-Ray Conf. (Salt Lake City), Vol. 6, ed. B. L. Dingus, D. B. Kieda, & M. H. Salamon (Melville: AIP), 403
Falcone, A. D., et al. 1999, Astropart. Phys., 11, 283
Fowler, G. N., & Wolfendale, A. W. 1961, Handbuck der Physik, Vol. 46/1 (Berlin: Springer), 312
Gosling, J. T. 1993, J. Geophys. Res., 98, 18937
Hayakawa, S. 1969, Cosmic Ray Physics (New York: Wiley)
Heck, D., Knapp, J., Capdevielle, J. N., Schatz, G., & Thouw, T. 1998, Corsika: A Monte Carlo Code to Simulate Extensive Air Showers (Rep. FZKA-6019; Univ. Karlsruhe Inst. Kernphys.)
Kahler, S. W. 1992, ARA&A, 30, 113
———. 1994, ApJ, 428, 837
Leblanc, Y., Dulk, G. A., Vourlides, A., & Borgeret, J. L. 2001, J. Geophys. Res., 106, 301
Lee, M. A. 1991, in Proc. 22d Int. Cosmic-Ray Conf. (Dublin), vol. 5, ed. M. Cawley et al. (Dublin: Dublin Inst. Advanced Studies), 293
———. 1997, in Coronal Mass Ejections, ed. N. Crooker, J. Joselyn, & J. Feynman (Monogr. 99; Washington: Am. Geophys. Union), 227
———. 2000, in AIP Conf. Proc. 528: Acceleration and Transport of Energetic Particles Observed in the Heliosphere, ed. R. A. Mewaldt et al. (Melville: AIP), 3
Lee, M. A., & Ryan, J. M. 1986, ApJ, 303, 829
Lockwood, J. A., Debrunner, H., & Ryan, J. M. 1999, Astropart. Phys., 12, 97
Lovell, J. L., Duldig, M. L., Humble, J. E. 1998, J. Geophys. Res., 103, 23733
Lovell, J. L., Duldig, M. L., Humble, J. E., Shea, M. A., Smart, D. F., & Flückiger, E. O. 2002, Adv. Space Res., 30, 1045
Maia, D., Vourlidas, A., Pick, M., Howard, R., Schwenn, R., Magalhães, A. 1999, J. Geophys. Res., 104, 12507
Mason, G. M., et al. 1999, Geophys. Res. Lett., 26, 141
McCullough, J. F., et al. 1999, in Proc. 26th Int. Cosmic-Ray Conf. (Salt Lake City), Vol. 2, ed. B. L. Dingus, D. B. Kieda, & M. H. Salamon (Melville: AIP), 369
Meyer, P., Parker, E. N., & Simpson, J. A. 1956, Phys. Rev., 104, 768
Möbius, E., et al. 1999, Geophys. Res. Lett., 26, 145
Parker, E. N. 1957, Phys. Rev., 107, 830
Reames, D. V. 1999, Space Sci. Rev., 90, 413
Ryan, J. M., et al. 1999, in Proc. 26th Int. Cosmic-Ray Conf. (Salt Lake City), Vol. 6, ed. B. L. Dingus, D. B. Kieda, & M. H. Salamon (Melville: AIP), 378
———. 2000, in AIP Conf. Proc. 528, Acceleration and Transport of Energetic Particles Observed in the Heliosphere, ed. R. A. Mewaldt et al. (Melville: AIP), 197
Sato, J., Masuda, S., Kosugi, T., & Sakao, T. 2000, Adv. Space Res., 26(3), 501
Simpson, J. A. 1957, Ann. IGY, part 7 (London: Pergamon)
Sullivan, G., et al. 2001, in Proc. 27th Int. Cosmic-Ray Conf. (Hamburg), Vol 7, ed. M. Simon, E. Lorenz, & M. Pohl (Katlenburg-Lindau: Copernicus Gesellschaft), 2773
Yoshimori, M., Suga, K., Shiozawa, A., Nakayama, S., & Takeda, H. 2000a, in AIP Conf. Proc. 528, Acceleration and Transport of Energetic Particles Observed in the Heliosphere, ed. R. A. Mewaldt et al. (Melville: AIP), 189
———. 2000b, in ASP Conf. Ser. 206, High Energy Solar Physics, Anticipating HESSI, ed. R. Ramaty & N. Mandzhavidze (San Francisco: ASP), 393
Zank, G. P., Rice, W. K. M., & Wu, C. C. 2000, J. Geophys. Res., 105, 25079
Zhang, J., Dere, K. P., Howard, R. A., Kundu, M., R., & White, S. M. 2001, ApJ, 559, 452